

A versatile apparatus for inverse and direct kinematic analysis of 3RRR planar parallel mechanisms

F Buium¹, D Leohchi¹, S Alaci² and C Duca¹

¹Mechanical Engineering, Mechatronics and Robotics Department, “Gheorghe Asachi” Technical University of Iasi, Iasi, Romania

²Mechanics and Technologies Department, “Stefan cel Mare” University of Suceava, Romania

E-mail: fbuium@gmail.com

Abstract. The paper presents an approach containing a package of several integrated programs, each of them being devoted to one of the principal problems regarding 3RRR planar parallel mechanisms: workspace, forward and direct kinematics and singularities problem. In order to perform workspaces coordinates and forward kinematics was used classical procedures, widespread and known in technical literature. For direct kinematics and singularities study, we used classical procedures also, but applied in a particular ways, related to each of them. Thereby, the proposed programs package represents a useful instrument in practical goals, one of them being didactical process of students’ instruction in engineering, but also for research and design purposes. The paper is a refined and a extended research of an older one [24].

1. Introduction

Together with extensive research of parallel mechanisms, it became clear that they present a series of incontestable advantages, as: higher structure stiffness, higher movements precision, fast response, increasing speeds, increasing working loads, and decreasing links mass. However they have a very important disadvantage, the presence of singularity points inside its workspace. This merely disadvantage drastically limits its applications [1-24].

Because the planar 3-RRR parallel mechanism determined a great interest in latest scientific literature, in this paper we do not insist about the exhaustively treated theoretically aspects, they will be pointed out only. Thus, workspace determining and forward kinematics was done using classical methods and mathematical apparatus from literature. In order to perform direct kinematics and singularities study we solved these fundamental and classically expressed problems, using certain, and special procedures with original character.

For each enumerated problem (workspace, forward and direct kinematics and singularities), a set of correlated computing programs was drew up, that allows to obtain numerical results [1-24].

2. Theoretical considerations

Let consider a planar mechanism shown in figure 1, consisting of two platforms: mobile $B_1B_2B_3$ platform and fixed one $O_1O_2O_3$. Without loosing of generality, it was supposed both platforms as equilateral triangles, $B_1B_2 = B_2B_3 = B_1B_3 = b$ and $O_1O_2 = O_2O_3 = O_1O_3 = L$, proximal links O_iA_i are equal ($O_iA_i = l_1, i = \overline{1,3}$) and also equal are distal links A_iB_i ($A_iB_i = l_2, i = \overline{1,3}$). The end-effector is



located in point M – the centre of equilateral triangle $B_1B_2B_3$. This point is determined by lengths s_i , $\bar{s}_i = \overline{B_iM}$, $i = \overline{1,3}$.

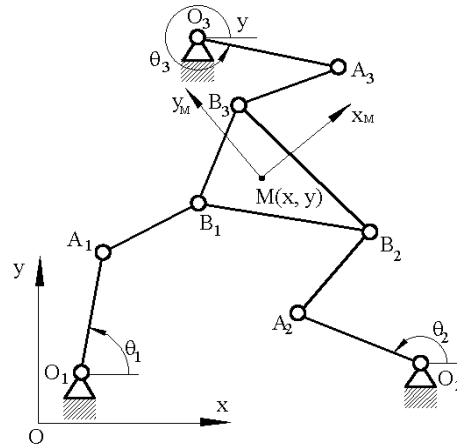


Figure 1. The 3RPR mechanism [4].

In order to solve the above mentioned problems regarding this mechanism, certain notations related to figure 1 were introduced: Oxy - a fixed referential system tied of fixed $O_1O_2O_3$ platform; Mx_My_M - a mobile system belonging to mobile $B_1B_2B_3$ platform; $q = [x, y, \varphi]$ - the input parameters, representing rectangular coordinates x, y of the end-effector in fixed referential system and φ - orientation of mobile platform, measured between Ox and Mx_M axes; $\Theta = [\theta_1, \theta_2, \theta_3]$ - angular positions of proximal (actuated) links; $\bar{o}_i = \overline{OO_i}$ - the position vectors of fixed actuated joints O_i ; $\bar{r}_i = \overline{O_iB_i}$, $\bar{v}_i = \overline{OM}$, $\bar{s}_i = \overline{MB_i}$.

For the studied mechanism, can be written following relation, based on figure 1,

$$\bar{r}_i = \bar{v} + R \cdot \bar{s}_i - \bar{o}_i, \tag{1}$$

where $R = \begin{pmatrix} \cos \varphi & -\sin \varphi \\ \sin \varphi & \cos \varphi \end{pmatrix}$ is the revolute matrix of centre M and radius s_i .

2.1. Workspace and IKP

Because these two problems were wide treated in literature, in this paper they are shortly presented. Thus, after squaring relation (1), the position vector of any workspace point can be expressed as:

$$\|\bar{r}_i\| = \left\{ \left[\begin{pmatrix} x \\ y \end{pmatrix} + \begin{pmatrix} \cos \varphi & -\sin \varphi \\ \sin \varphi & \cos \varphi \end{pmatrix} \cdot \begin{pmatrix} x_{Bi}^M \\ y_{Bi}^M \end{pmatrix} - \begin{pmatrix} x_{Oi} \\ y_{Oi} \end{pmatrix} \right]^T \left[\begin{pmatrix} x \\ y \end{pmatrix} + \begin{pmatrix} \cos \varphi & -\sin \varphi \\ \sin \varphi & \cos \varphi \end{pmatrix} \cdot \begin{pmatrix} x_{Bi}^M \\ y_{Bi}^M \end{pmatrix} - \begin{pmatrix} x_{Oi} \\ y_{Oi} \end{pmatrix} \right] \right\}^{\frac{1}{2}}, \tag{2}$$

where x_{Bi}^M, y_{Bi}^M are the vertexes B_i coordinates in mobile system and x_{Oi}, y_{Oi} - the fixed points coordinates reported to fixed system.

Writing relation (2) for situation when distal and proximal links overlaps or are in extension, i.e. $\|\bar{r}_i\| = |l_1 \mp l_2|$ and after some calculations, it obtains the equations limiting mechanism workspace, as a mathematical gather of six circles with variable centres, concentric two by two:

$$\left(x + x_{Bi}^M \cos \varphi - y_{Bi}^M \sin \varphi - x_{Oi}\right)^2 + \left(y + y_{Bi}^M \sin \varphi + x_{Bi}^M \cos \varphi - y_{Oi}\right)^2 = (l_1 \mp l_2)^2. \quad (3)$$

Centres coordinates are:

$$a_i = -x_{Bi}^M \cos \varphi + y_{Bi}^M \sin \varphi + x_{Oi}, \quad b_i = -x_{Bi}^M \sin \varphi - y_{Bi}^M \cos \varphi + x_{Oi}. \quad (4)$$

In order to solve the forward kinematic problem it writes an equation, according to figure 1:

$$\overline{A_i B_i} = \overline{OM} + R \cdot \overline{s_i} - \overline{O_i A_i} - \overline{OO_i}. \quad (5)$$

Applying law of cosines in $O_i A_i B_i$ triangles, squaring equation (5), after accomplishing calculations, it can write the input rotation angles $\Theta = [\theta_1, \theta_2, \theta_3]$:

$$\theta_i = 2 \cdot \tan^{-1} \left(\frac{y - b_i + d_i \sqrt{\Delta_i}}{x + K_i - a_i} \right), \quad (6)$$

where, $d_i = \pm 1$ is an coefficient depending on the mechanism assembling mode (of eight possible),

$$K_i = \frac{1}{2l_1} \left[(x - a_i)^2 + (y - b_i)^2 + l_1^2 - l_2^2 \right] \text{ and } \Delta_i = (x - a_i)^2 + (y - b_i)^2 - K_i.$$

2.2. DKP and singularities

As was mentioned above, for these two important problems were used knowledge wide developed in technical literature, but applied in a particular ways. Just this particularity contributes to versatile character of the proposed approach. So, to solve DKP, it supposes angular positions of proximal (actuated) links $\Theta = [\theta_1, \theta_2, \theta_3]$ as input data, it find to determine as output parameters $q = [x, y, \varphi]$ - the end-effector coordinates and the mobile platform orientation.

This problem can be approached two ways: firstly, knowing instantaneous positions of the proximal links, three ends x_{Ai}, y_{Ai} , can be written six equations, expressing the length l_i of proximal links and the side b of mobile platform:

$$\begin{aligned} (x_{B1} - x_{A1})^2 + (y_{B1} - y_{A1})^2 &= l_2^2 \\ (x_{B2} - x_{A2})^2 + (y_{B2} - y_{A2})^2 &= l_2^2 \\ (x_{B3} - x_{A3})^2 + (y_{B3} - y_{A3})^2 &= l_2^2 \\ (x_{B2} - x_{B1})^2 + (y_{B2} - y_{B1})^2 &= b^2 \\ (x_{B3} - x_{B2})^2 + (y_{B3} - y_{B2})^2 &= b^2 \\ (x_{B3} - x_{B1})^2 + (y_{B3} - y_{B1})^2 &= b^2. \end{aligned} \quad (7)$$

This system with unknowns x_{Bi}, y_{Bi} , $i=1,2,3$ can be solved by numerical methods, taking into account appropriate initial conditions. For first iteration may be considered values obtained graphically e.g., and for the others ones can be considered as initial conditions, the output values from the previous step.

Other method to solve this problem (used in our research), takes into account the four bar linkage with variable basis $A_2 B_2 B_3 A_3$ (figure 1, figure 2). This linkage is supposed to have variable basis (length $A_2 A_3$) and actuated joint A_2 , the independent (input) parameter is angle φ_2 and output parameters – angles $\varphi_b, \varphi_3, \varphi$.

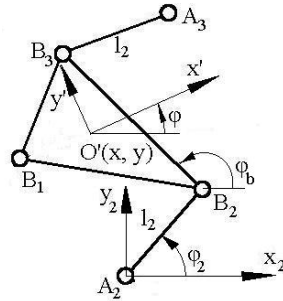


Figure 2. The $A_2 - B_2 - B_3 - A_3$ kinematic chain, [24].

Let consider the vector contour $A_2B_2B_3A_3$ (figure 2), and aided it, following vector equation can be written:

$$\overline{A_2B_2} + \overline{B_2B_3} + \overline{B_3A_3} + \overline{A_3A_2} = 0. \tag{8}$$

Projecting this equation on $A_2x_2y_2$ system, with origin in A_2 and axes being parallel to general fixed system Oxy , it obtains:

$$l_2 \cos \varphi_2 + b \cos \varphi_b + l_2 \cos \varphi_3 = x_{A_3} - x_{A_2}, \quad l_2 \sin \varphi_2 + b \sin \varphi_b + l_2 \sin \varphi_3 = y_{A_3} - y_{A_2}, \tag{9}$$

with imposed φ_2 and unknowns $\varphi_b, \varphi_3, x_{B1}, x_{B1}$.

Introducing in $a = x_{A_3} - x_{A_2} - l_2 \cos \varphi_2$ and $c = y_{A_3} - y_{A_2} - l_2 \sin \varphi_2$, in (9), this becomes:

$$\begin{cases} l_2 \cos \varphi_3 + b \cos \varphi_b = a \\ l_2 \sin \varphi_3 + b \sin \varphi_b = c \end{cases} \quad \text{or} \quad \begin{cases} l_2 \cos \varphi_3 = a - b \cos \varphi_b \\ l_2 \sin \varphi_3 = c - b \sin \varphi_b. \end{cases} \tag{10}$$

Squaring both sides of equation (10) and suitable arranging its terms, we have:

$$a \cos \varphi_b + c \sin \varphi_b - \frac{a^2 + b^2 + c^2 - l_2^2}{2b} = 0. \tag{11}$$

Writing down $\frac{a^2 + b^2 + c^2 - l_2^2}{2b} = d$, $\tan \frac{\varphi_2}{2} = t$, $\sin \varphi_b = \frac{2t}{1+t^2}$, $\cos \varphi_b = \frac{1-t^2}{1+t^2}$, equation (11) takes following form:

$$(a+d) \cdot t^2 - 2c \cdot t - (a-d) = 0. \tag{12}$$

If $\Gamma = c^2 + a^2 - d^2 \geq 0$, then equation (12) has two real solutions:

$$t_{1,2} = \frac{c \pm \sqrt{\Gamma}}{a+d} \quad \text{and} \quad \varphi_b = 2 \tan^{-1}(t). \tag{13}$$

Then, $\begin{cases} x_{B1} = l_2 \cdot \cos \varphi_2 + b \cdot \cos(\varphi_b + 60^\circ) \\ y_{B1} = l_2 \cdot \sin \varphi_2 + b \cdot \sin(\varphi_b + 60^\circ) \end{cases}$, $\varphi = \varphi_b - \frac{2\pi}{3}$ with respect the condition $A_1B_1 \cong l_2$ and

$$x_M = x_{A_2} + l_2 \cos \varphi_2 + s \cdot \cos\left(\varphi_b + \frac{\pi}{6}\right), \quad y_M = y_{A_2} + l_2 \sin \varphi_2 + s \cdot \sin\left(\varphi_b + \frac{\pi}{6}\right). \tag{14}$$

2.3. Singularities problem

Considering function,

$$F_i(x,y) = (x + x_{Bi}^M \cos \varphi - y_{Bi}^M \sin \varphi - x_{Oi} - l_i \cos \theta_i)^2 - (y + x_{Bi}^M \sin \varphi + y_{Bi}^M \cos \varphi - y_{Oi} - l_i \sin \theta_i)^2 - l_2^2,$$

as an implicit three dimensional function of a three dimensional variable $q=[x,y,\varphi]$, so that $F(\Theta,q) = 0$. After differentiating this relation with respect to time it obtains an expression between input and output velocities $J_q \cdot \dot{q} + J_\theta \cdot \dot{\Theta} = 0$. From this matrix equation it can write the ΔJ_q jakobian determinant of J_q matrix. Putting $\Delta J_q = 0$, singularities of 2nd type can be studied [1-5].

The problem shortly presented, (workspace, forward and direct kinematics, singularities) can be studied using the proposed programs package, having the following structure (figure 3):

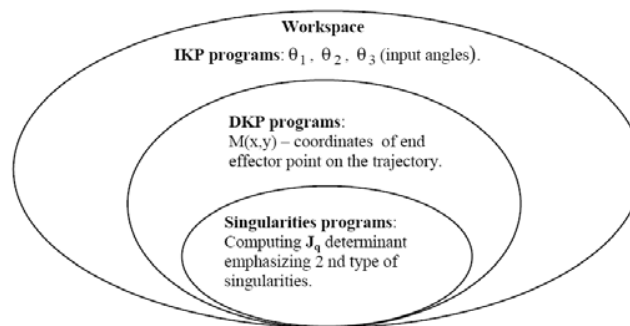


Figure 3. Programs package general structure.

Figure 4 indicates also the order which must respect in solving these problems, taking into account that output data from a problem ought to be input data for other.

3. Numerical exemplifying

In this section, some numerical results after running proposed programs will be presented. In each case were indicated dimensional parameters of mechanism and diagrams significances.

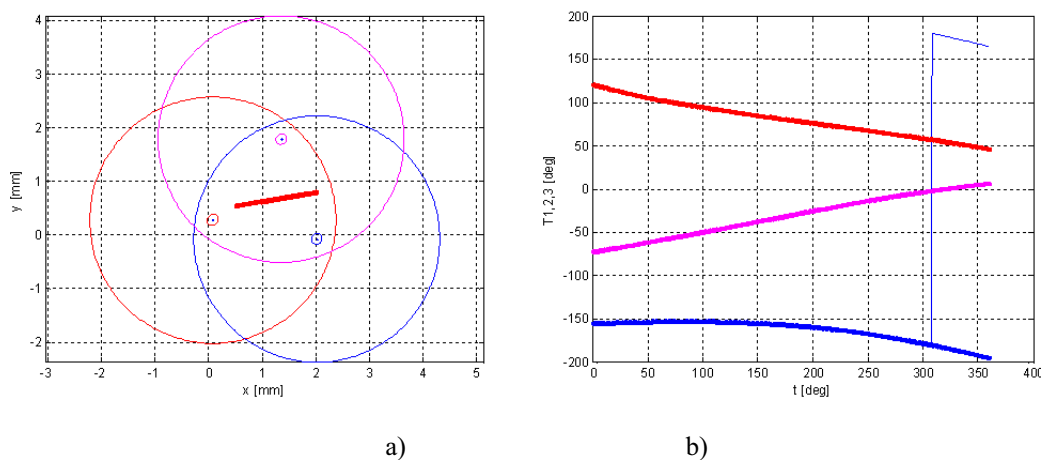


Figure 4. a) Workspace and end effector trajectory; b) Driving links angles as result of IKP; $L=2.3$; $l_1=1.1$; $l_2=1.2$; $b=0.5$; $\varphi = \pi / 4$; linear trajectory.

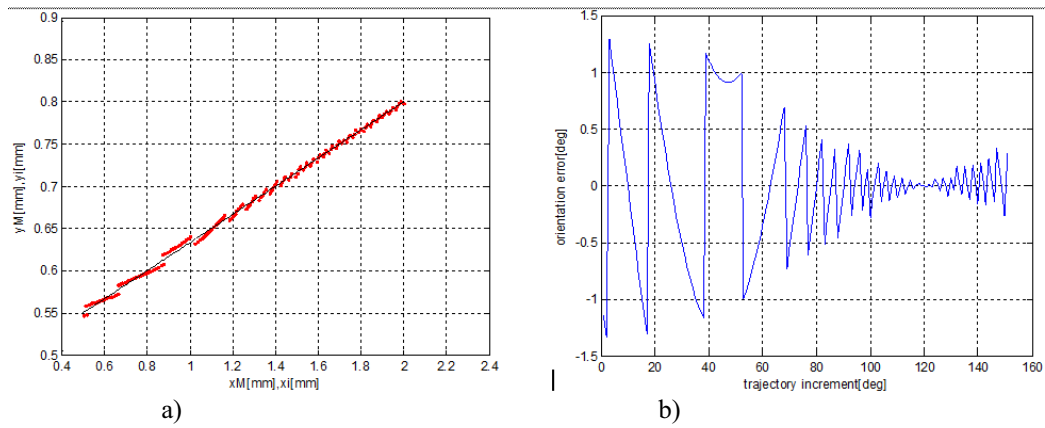


Figure 5. a) DKP result, red – obtained and black – etalon trajectories; b) Mobile platform angle error; $L=2.3$; $l_1=1.1$; $l_2=1.2$; $b=0.5$; $\varphi = \pi/4$; linear trajectory.

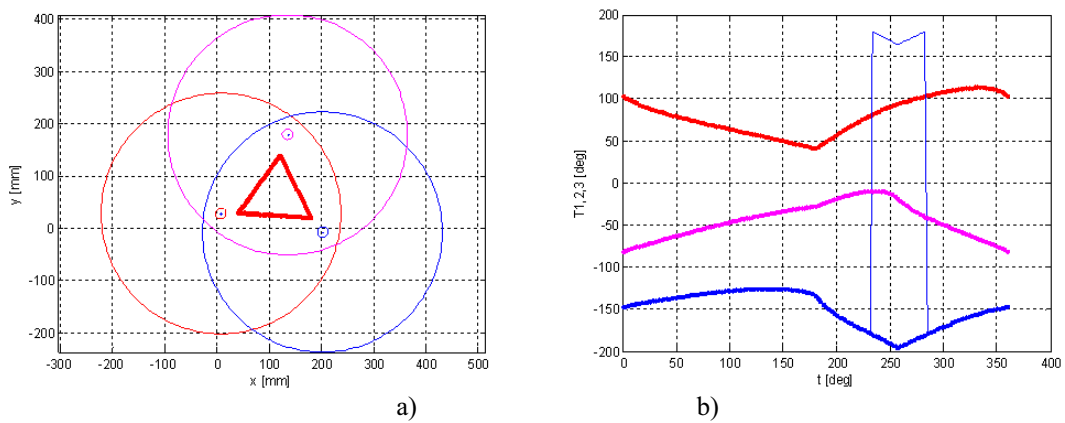


Figure 6. a) Workspace and end effector trajectory; b) Driving links angles as result of IKP; $L=2.3$; $l_1=1.1$; $l_2=1.2$; $b=0.5$; $\varphi = \pi/4$; triangular trajectory.

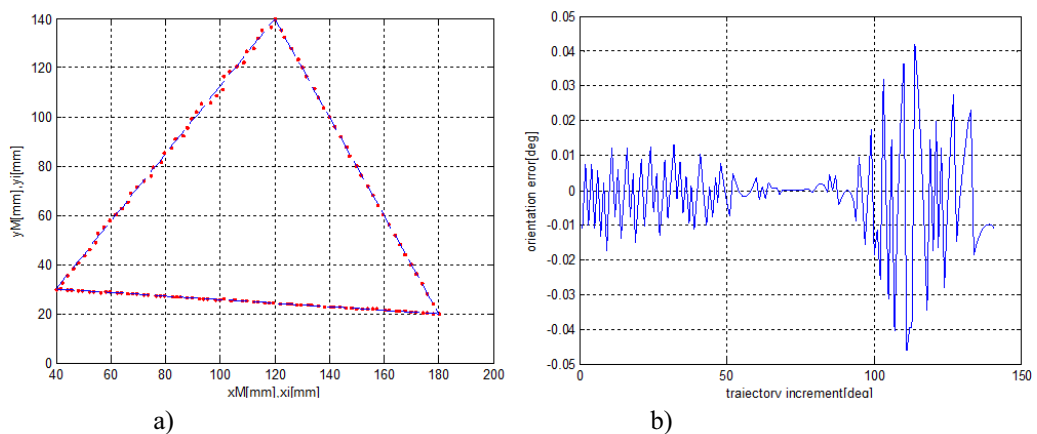


Figure 7. a) DKP result, red – obtained and black – etalon trajectories; b) Mobile platform angle error; $L=2.3$; $l_1=1.1$; $l_2=1.2$; $b=0.5$; $\varphi = \pi/4$; triangular trajectory.

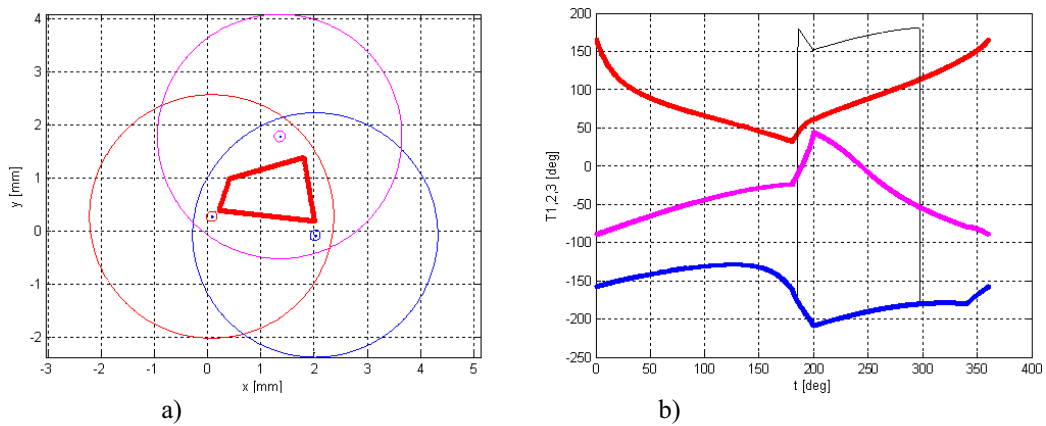


Figure 8. a) Workspace and end effector trajectory; b) Driving links angles as result of IKP; $L=2.3$; $l_1=1.1$; $l_2=1.2$; $b=0.5$; $\varphi = \pi/4$; quadrilateral trajectory.

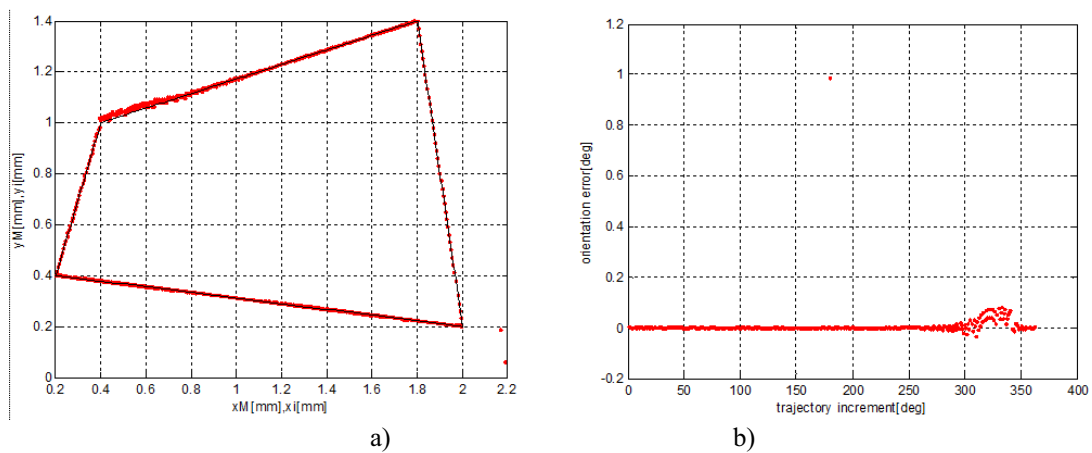


Figure 9. a) DKP result, red – obtained and black – etalon trajectories; b) Mobile platform angle error; $L=2.3$; $l_1=1.1$; $l_2=1.2$; $b=0.5$; $\varphi = \pi/4$; quadrilateral trajectory.

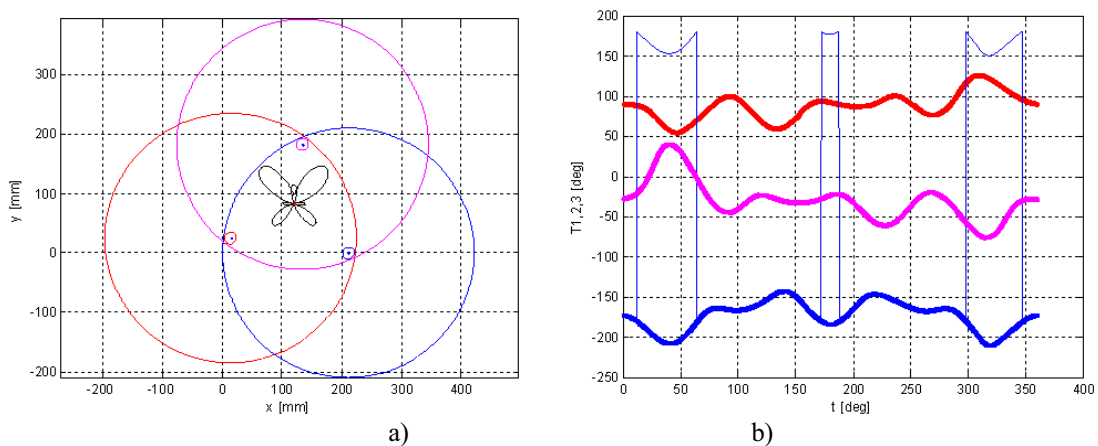


Figure 10. a) Workspace and end effector trajectory; b) Driving links angles as result of IKP; $L=2.4$; $l_1=1$; $l_2=1.1$; $b=0.5$; $\varphi = \pi/6$; complex ('butterfly' curve) trajectory.

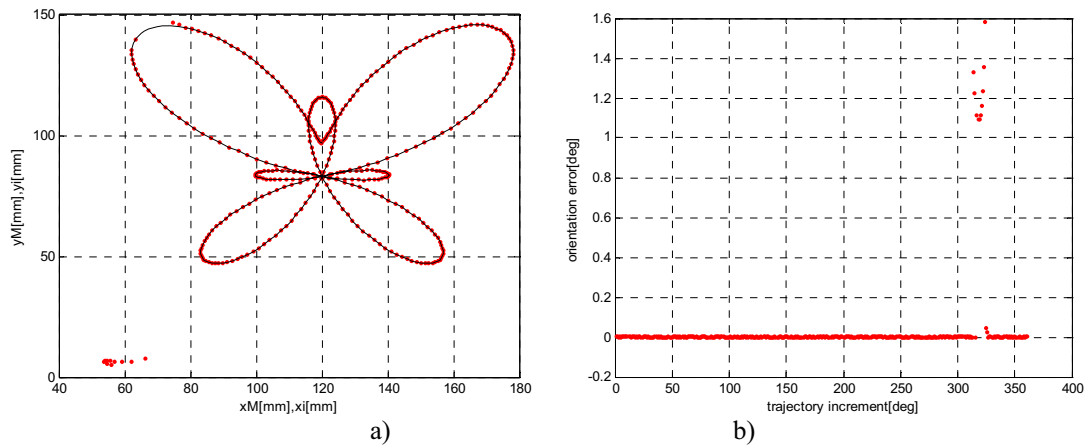


Figure 11. a) DKP result, red – obtained and black – etalon trajectories; b) Mobile platform angle error; $L=2.4$; $l_1=1$; $l_2=1.1$; $b=0.5$; $\varphi = \pi / 6$; complex ('butterfly' curve) trajectory.

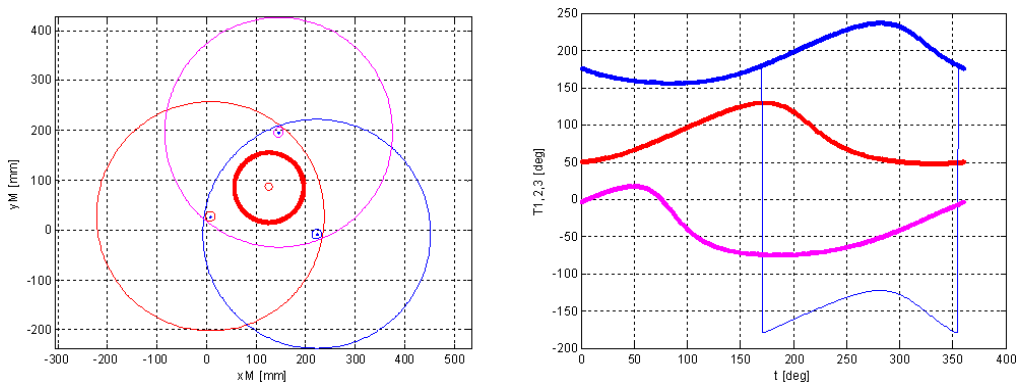


Figure 12. a) Workspace and end effector trajectory; b) Driving links angles as result of IKP; $L=2.5$; $l_1=1.1$; $l_2=1.2$; $b=0.5$; $\varphi = \pi / 4$; circular trajectory.

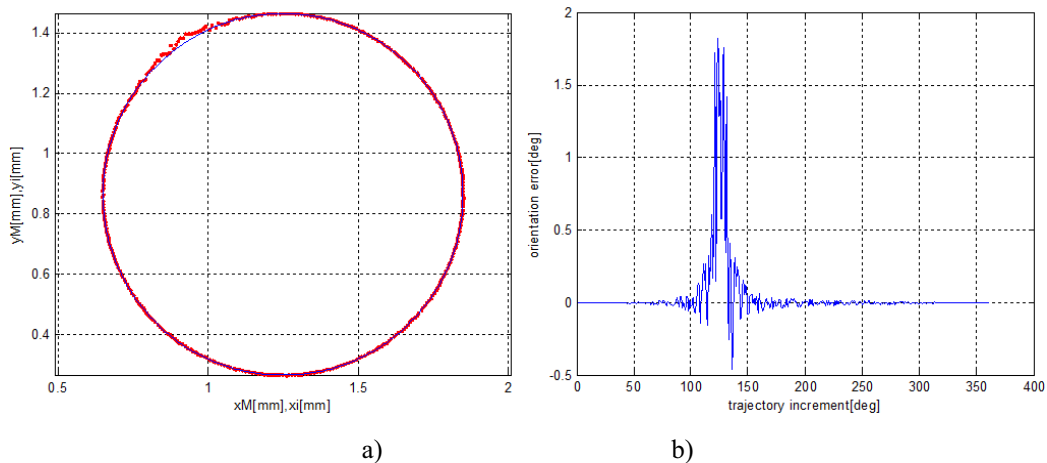


Figure 13. a) DKP result, red – obtained and black – etalon trajectories; b) Mobile platform angle error; $L=2.5$; $l_1=1$; $l_2=1.2$; $b=0.5$; $\varphi = \pi / 4$; circular trajectory.

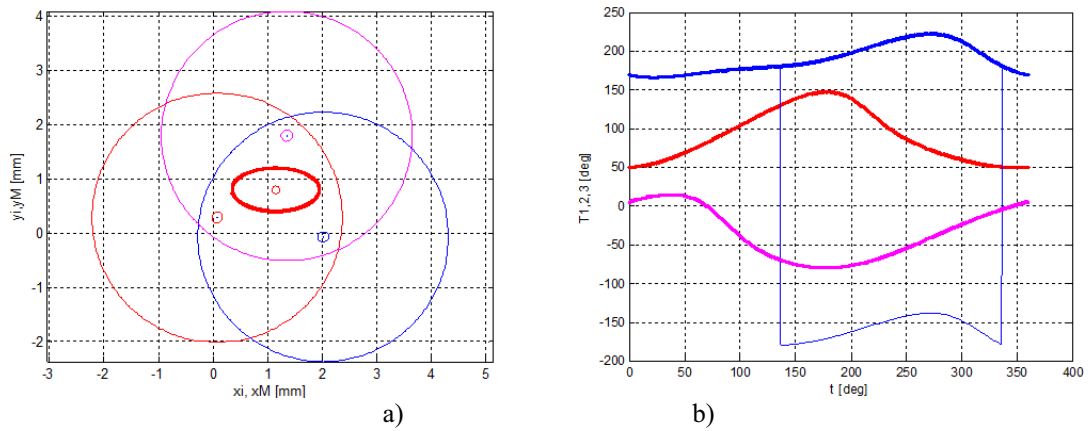


Figure 14. a) Workspace and end effector trajectory; b) Driving links angles as result of IKP; $L=2.3$; $l_1=1.1$; $l_2=1.2$; $b=0.5$; $\varphi = \pi/4$; elliptic trajectory.

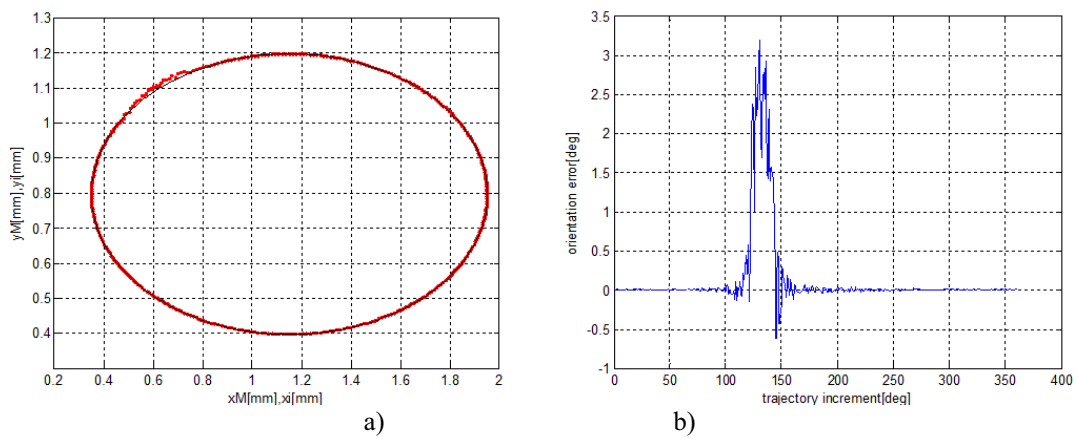


Figure 15. a) DKP result, red – obtained and black – etalon trajectories; b) Mobile platform angle error; $L=2.3$; $l_1=1$; $l_2=1.2$; $b=0.5$; $\varphi = \pi/4$; circular trajectory.

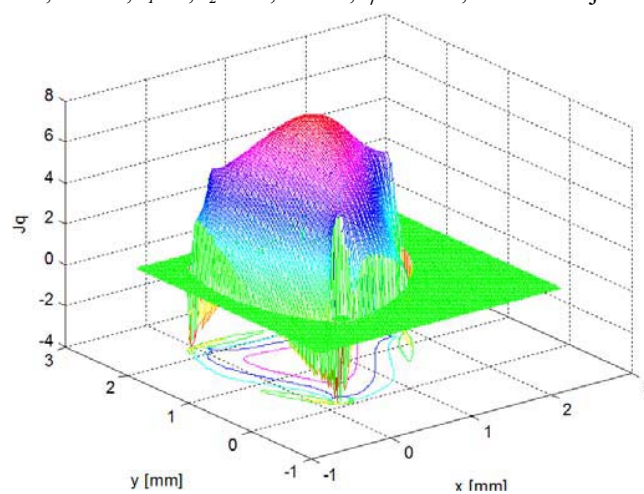


Figure 16. J_q determinant, emphasizing singularities zones; $L=2.4$; $l_1=1$; $l_2=1.1$; $b=0.5$; $\varphi = \pi/6$.

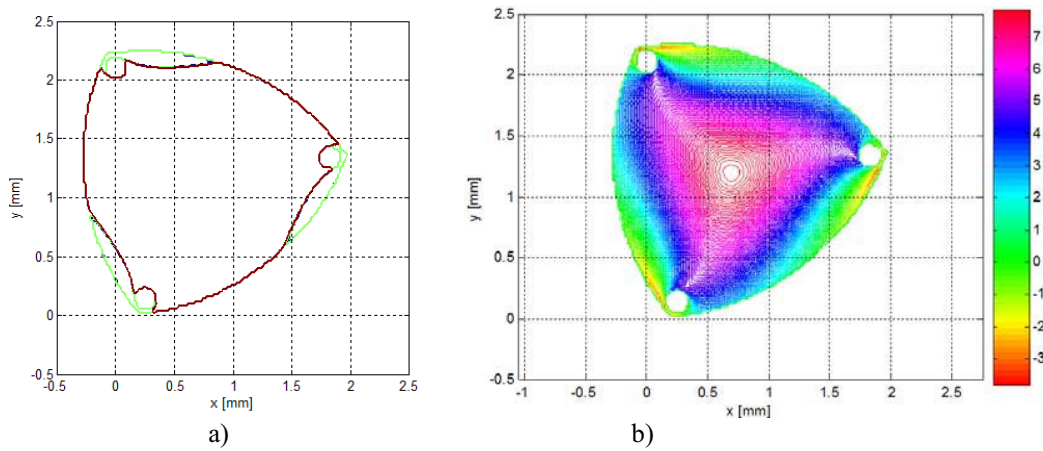


Figure 17. Workspaces contour with emphasized singularities of both types 1st and 2nd, a) using level curves and b) using color map; $L=2.4; l_1=1; l_2=1.1; b=0.5 \varphi = \pi / 6$.

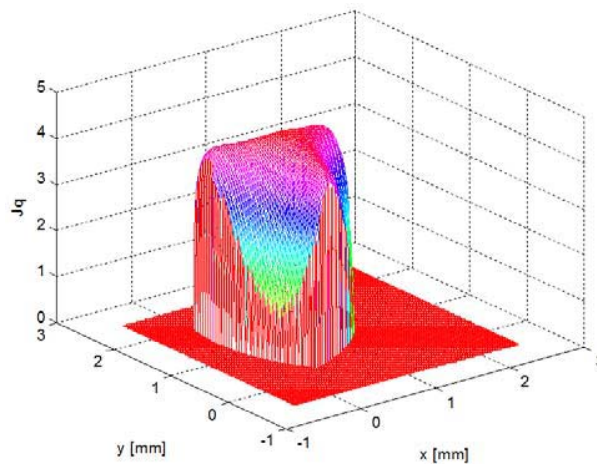


Figure 18. J_q determinant, emphasizing singularities zones; $L=2.4; l_1=1; l_2=1.1; b=0.5; \varphi = \pi / 2$.

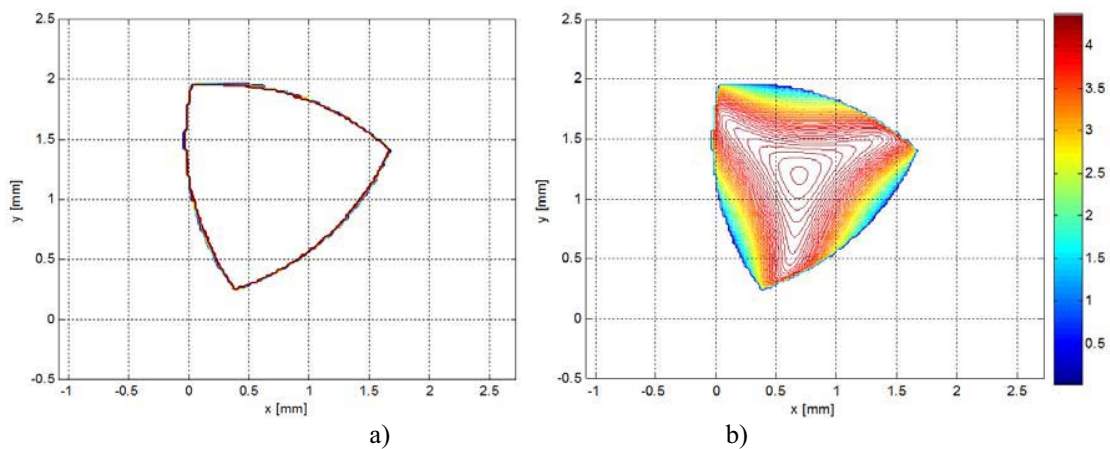


Figure 19. Workspaces contour with emphasized singularities of both types 1st and 2nd, a) using level curves and b) using color map; $L=2.4; l_1=1; l_2=1.1; b=0.5 \varphi = \pi / 2$.

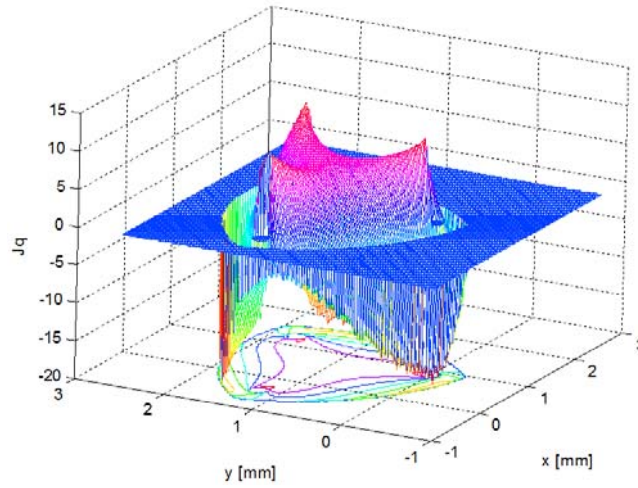


Figure 20. J_q determinant, emphasizing singularities zones; $L=2$; $l_1=1$; $l_2=1.1$; $b=1.5$; $\varphi = \pi/3$.

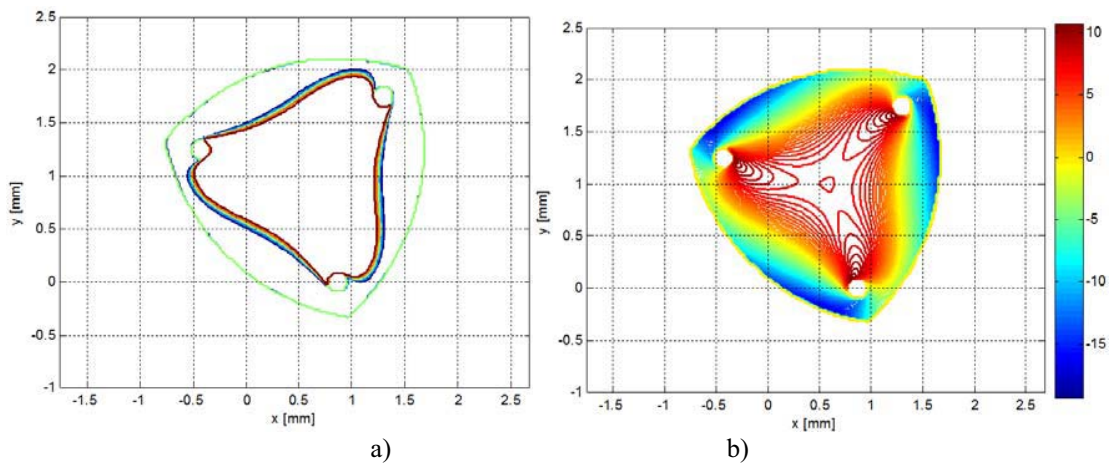


Figure 21. Workspaces contour with emphasized singularities of both types 1st and 2nd, a) using level curves and b) using color map; $L=2$; $l_1=1$; $l_2=1.1$; $b=1.5$ $\varphi = \pi/3$.

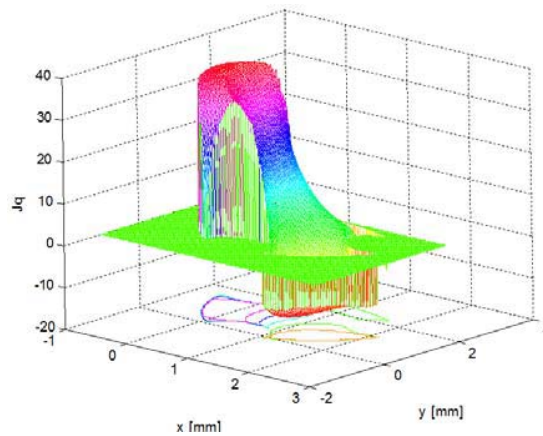


Figure 22. J_q determinant, emphasizing singularities zones; $L=2.5$; $l_1=1$; $l_2=1.5$; $b=1$; $\varphi = \pi/3$.

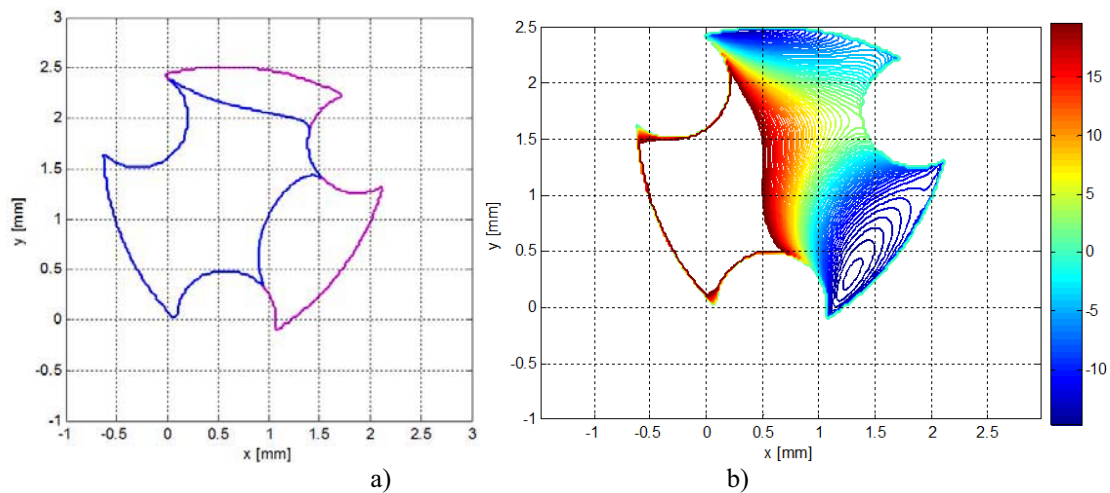


Figure 23. Workspaces contour with emphasized singularities of both types 1st and 2nd, a) using level curves and b) using color map; $L=2.5$; $l_1=1$; $l_2=1.5$; $b=1$ $\varphi = \pi/3$, $d_1 = -1, d_2 = 1, d_3 = 1$.

In this section were presented numerical results after running above mentioned programs. Were taken into consideration some simple end effector trajectories (line, triangle, quadrilateral, circle, ellipse and a more complex one – ‘butterfly curve’). For each of them were drawn workspace contour as intersection of three annular zones. Inside workspace was shown end effector trajectory located in the center of mobile platform. Then, after IKP running were obtained and drawn, proximal (actuated) links positions $\Theta = [\theta_1, \theta_2, \theta_3]$ as function of time or of the incremental angular parameter used to define trajectory. Here, because of using arctangent function which is defined on interval $\left(-\frac{\pi}{2}, \frac{\pi}{2}\right)$

only, some mathematical transformations needed. The problem consists in fact that discontinuities in $\Theta = [\theta_1, \theta_2, \theta_3]$ diagrams comes from arctangent using but also from mechanism kinematics. As result of DKP program running, angular parameters of actuated links were verified. Using fine divisions of the independent parameters, a good correspondence were obtained between prescribed and real trajectories, excepting cases where trajectory intersects singularity zones of both types 1st and 2nd. This fact can be noticed in some diagrams.

All considered figures were obtained for one only assembling mode of actuated (proximal) links (still seven cases from the all eight may be taken into consideration).

4. Conclusions

This paper represents an extended, refined and a thoroughgoing study, starting from an elder one [24]. Following this research, an interdependent programs package was approached, in order to depict kinematics of the 3RRR planar mechanisms. Thus, mechanism workspace, forward and direct kinematics and singularities problem can be performed using this package as an specialized instrument.

This instrument can be used by engineer students in learning process and also by designer engineers in their applications, without a very specialization in the field.

This research need still more refinement, in each it compartments as in assembly regarded and taking into account complex relationship between it parts. Especially, it will pay attention about direct kinematics and singularities.

The proposed software package has a versatile character, allowing to study and verify a large number of mechanisms from treated category.

5. References

- [1] Merlet, J-P., Le robots paralleles, 2e edition revue et augmentee, *Editions Hermes*, Paris, 1997.
- [2] Doroftei, I., Singularity analysis of a 3RRR planar parallel robot I -Theoretical aspects, *Buletinul Institutului Politehnic din Iași, Tom LIV(LVIII), Fas. 1, 2008, Secția Construcții de Mașini*, Iași, pp.465-472.
- [3] Doroftei, I., Singularity analysis of a 3RRR planar parallel robot II - Physical significance, *Buletinul Institutului Politehnic din Iași, Tom LIV(LVIII), Fas. 1, 2008, Secția Construcții de Mașini*, Iași, pp.473-480.
- [4] Arsenault, M., Boudreau, R., The synthesis of three-degree-of-freedom planar mechanism with revolute joints (3-RRR) for an optimal singularity-free workspace, *Journal of Robotic Systems* 21(5), 259-274 (2004).
- [5] Bonev, I. Geometric analysis of planar mechanisms, *PhD thesis*, Departament de Genie Mecanique, Faculte des Sciences et de Genie, Universite Laval, Quebec (2002).
- [6] Zlatanov, D. Generalized singularity analysis of mechanisms, *PhD thesis*, Departament of Mechanical and Industrial Engineering, University of Toronto (1988).
- [7] Merlet, J-P., Parallel manipulators: state of the art and perspectives, <http://www.sop.inria.fr/saga/personnel/merlet/merlet.html>, Inst. Nat.de Rech. en Inf. et en Auto, France, (1999).
- [8] Merlet, J-P., Parallel Robots, *Kluwer Academic Publishers*, (2000).
- [9] Merlet, J-P., Gosselin, C.M., Mouly, N., Workspaces of planar manipulators, *Mechanism and Machine Theory*, 33(1-2), (1998), pp. 7-20.
- [10] Kumar, V., Characterization of workspaces of parallel manipulators, ASME, *Journal of Mechanical Design* 114(3), (1992), pp. 368-375.
- [11] Gosselin, C.M. and Angeles, J., The optimum kinematic design of a planar three degree of freedom parallel manipulator, *ASME J. Mech Transm Autom Des* 110:(1), (1988), pp.35-41.
- [12] J.-P. Merlet, Designing a parallel manipulator for a specific workspace, *Int J Robot Res* 16:(4), (1977), pp. 545-556.
- [13] Gosselin, G.M. and Wang, J., Singularity loci of planar parallel manipulators with revolute joints, *Robot Auton Syst* 21:(4) (1997), pp. 377-398.
- [14] Boudreau, R. and Gosselin, C.M., La synthese d'un plat-forme Gough-Stewart pour un espace atteignable prescript, *Mech Mach Theory* 36:(3) (2001), pp. 327-342.
- [15] Bonev, I.A. and Gosselin, C.M., Singularity loci of planar manipulators with revolute joint, *2nd Workshop on Computational Kinematics*, Seoul, South Korea, (2001), pp. 1964-1969.
- [16] Gosselin, C.M. and Angeles, J., Singularity analysis of close-loop kinematic chains, *IEEE Trans Robot Automom* 6(3) (1990), pp. 281-290.
- [17] Gosselin, C.M. and Angeles, J., A global performance index for the kinematic optimization of robotic manipulators, *ASME J Mech Des* 113:(13) (1991), pp. 220-226.
- [18] Sefroui, J. and Gosselin, C.M., On the quadratic nature of the singularity curves of planar three degree of freedom parallel manipulators, *Mech Mach Theory*, 30:(4) (1995), pp. 533-551.
- [19] Hunt, K.H., Kinematic geometry of mechanisms, *Oxford University press*, (1978) pp. 199-201.
- [20] Merlet, J.-P., Direct kinematic of planar parallel manipulators, *Proc. IEEE Int. Conf. on Robotics, Minneapolis, MN, April 1996*, pp. 3744-3749.
- [21] Daniali, H.R.M., Zsombor-Murray, P.J. and Angeles, J. Singularities analysis of planar parallel manipulators, *Mech. Mach. Theory* 30 (5), pp. 665-678.
- [22] Buium, Fl., Leohchi, D. Doroftei, I., A workspace characterization of the 3 RRR planar mechanism, *Applied Mechanics and Materials*, vol 658(2014), Trans Tech Publications, Switzerland doi 10.4028/ www.scientific.net/ AMM. 658.563, pp. 563-568.
- [23] Buium, Fl., Duca, C., Leohchi, D., Problems regarding singularities analysis of a 3 RRR parallel mechanism, *Applied Mechanics and Materials*, vol 658(2014), Trans Tech Publications, Switzerland doi 10.4028/ www.scientific.net/ AMM. 658.569, pp. 569-547.
- [24] Buium F, Leohchi, D, Duca CD, An IKP-DKP approach emphasizing singularities of 9R (3-RRR) mechanisms, *SYROM 2017*, Iassy 2nd nov. 2017.